

pH-Tunable Thermoresponsive PEO-Based Functional Polymers with Pendant Amine Groups

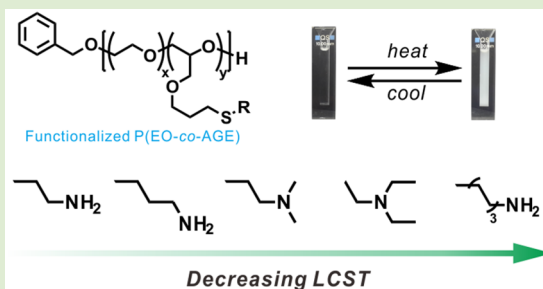
Joonhee Lee,[†] Alaina J. McGrath,[‡] Craig J. Hawker,^{*,‡} and Byeong-Su Kim^{*,†}

[†]Department of Chemistry, School of Natural Science, Ulsan National Institute of Science and Technology (UNIST), Ulsan 44919, Korea

[‡]Materials Research Laboratory, University of California Santa Barbara, Santa Barbara, California 93106, United States

Supporting Information

ABSTRACT: Thermoresponsive polymers exhibiting lower critical solution temperatures (LCSTs) in aqueous solution have garnered considerable attention for the development of smart materials. Herein, we report the synthesis and properties of pH-tunable thermoresponsive poly(ethylene oxide) (PEO)-based functional polymers bearing pendant amine groups with varying cloud points. Well-defined poly(ethylene oxide-co-allyl glycidyl ether) (P(EO-co-AGE)) copolymers were prepared via controlled anionic ring-opening copolymerization of ethylene oxide (EO) with 10 mol % of a functional allyl glycidyl ether (AGE) comonomer. Facile, modular thiol-ene click chemistry was then employed to introduce a library of different aminothiols as side chains to the initial P(EO-co-AGE) copolymer. Depending on the nature of the pendant amine groups (primary amine, dimethylamine, and diethylamine) and the hydrophobicity of the side chains (ethyl, propyl, and hexyl), the cloud points could be tuned from 44–100 °C under different pH conditions. This is the first systematic investigation into the effect of PEO copolymer side chains on cloud point, which opens up the opportunity to make new thermoresponsive polymers for a variety of smart material applications.



Polymers capable of responding to various environmental stimuli such as temperature,^{1–3} pH,⁴ light,⁵ and mechanical force⁶ have attracted significant attention, with applications ranging from environmental materials to biomedical devices. Thermoresponsive polymers, in particular, have been investigated for the development of smart materials due to their unique phase transition properties in aqueous solution, including lower critical solution temperature (LCST) and upper critical solution temperature (UCST).^{7–10} In particular, the lower critical solution temperature (LCST) is the temperature above which phase separation is observed, which coincides with decreasing polymer solubility.^{11,12} At low temperatures, LCST-type thermoresponsive polymers are soluble, owing to hydrogen bonding with the surrounding water molecules, resulting in restricted intra/intermolecular interactions between polymer chains. Upon heating, the hydrogen bonds are disrupted, and the polymer chains exhibit a phase transition, with solubility decreasing due to the disruption of the interactions between the polymer and the solvating water molecules. It has been suggested that the LCST is dependent on many external parameters, including monomer composition, the hydrophilic/hydrophobic balance, molecular weight, concentration, and the ionic species present.^{13–16} The ability to develop thermoresponsive polymers with a wide range of LCSTs that can be tuned depending on external stimuli is therefore of significant interest.^{17–20}

The most studied thermoresponsive polymer, poly(*N*-isopropylacrylamide) (PNIPAM), exhibits a clear phase transition at a LCST of 32 °C, close to body temperature.¹³ Water-soluble, nontoxic, and nonimmunogenic poly(ethylene oxide) (PEO) is another biologically important synthetic polymer that is widely used in biomedical applications.^{21–23} However, PEO's LCST (nearly 100 °C)²⁴ is too high for most biomedical applications, prompting studies on the LCST behavior of PEO-based polymers. These studies have tailored the LCST of PEO by introducing hydrophobic side chains to the PEO backbone or by the integration of new functional monomers.²⁵ As notable examples, a range of monomers containing hydrophobic side chains have been copolymerized with ethylene oxide (EO) to yield functional PEO derivatives exhibiting varying LCST values, including glycidyl methyl ether,²⁶ ethoxyl vinyl glycidyl ether,^{27,28} *N,N*-diisopropyl ethanol amine glycidyl ether,⁴ allyl glycidyl ether (AGE),²⁸ and *N,N*-dibenzyl amino glycidyl.^{28,29} Although the aforementioned functional monomers lead to modulation of the LCST, a major drawback of their use is the requirement of separate syntheses for each functional copolymer with varying comonomer contents. As a result, there is a significant time

Received: October 31, 2016

Accepted: November 30, 2016

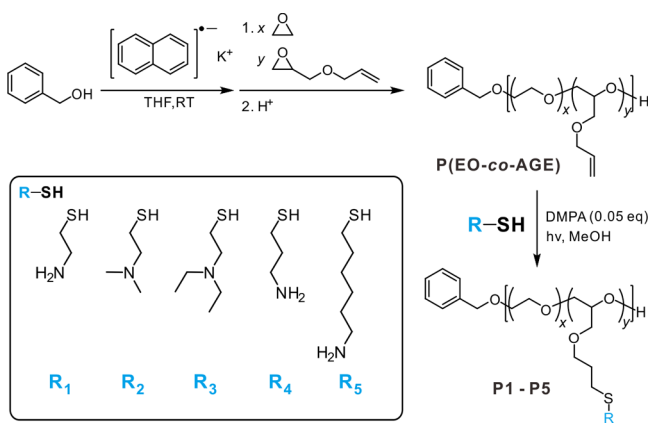
Published: December 2, 2016

and materials investment for the preparation of a library of materials with a range of LCST values.

As an alternative strategy, postpolymerization functionalization of a single PEO-based starting copolymer with a defined molecular weight, architecture, and polydispersity can be used to furnish a library of copolymers with varying LCSTs. In particular, PEO-based copolymers with functional allyl side chains offer a unique handle that is amenable to quantitative thiol–ene click chemistry, with prior work showing the successful controlled copolymerization of EO and AGE, followed by conjugation with multifunctional peptide units.³⁰ In addition to lowering the LCST, controlling the LCST behavior of PEO-based polymers with an external stimuli such as pH can offer new application opportunities.

Herein, we describe the synthesis of a series of thermoresponsive, functional PEO-based polymers bearing pendant amine groups via postpolymerization modification of P(EO-*co*-AGE) copolymers through thiol–ene coupling chemistry using five different aminothiols (R-SH, see Scheme 1),

Scheme 1. Synthesis of Amine-Functionalized PEO-Based Polymers, P1–P5, with Different Pendant Amine Groups (R₁–R₅)



including cysteamine (R₁), *N,N*-dimethylaminoethanethiol (R₂), *N,N*-diethylaminoethanethiol (R₃), 3-amino-1-propanethiol (R₄), and 6-amino-1-hexanethiol (R₅). This allowed a systematic investigation into the effect of PEO copolymer side chains on LCST behavior through varying the nature of the amine groups (primary R₁ vs tertiary R₂ and R₃), the length of the side chains (R₁, R₄, and R₅), and the pH. Generally, LCST behavior is determined qualitatively by measuring the cloud point temperature; this is the temperature that corresponds to the polymer solution optically changing from transparent to turbid.³¹ The modified functional copolymers, P1–P5, were successfully characterized by ¹H NMR and GPC analysis, with the resulting copolymers exhibiting significantly different, yet tunable LCST behavior under varying pH conditions. Lee and co-workers previously reported that the LCST of amine-functionalized poly(2-hydroxyethyl methacrylate) (PHEMA) was significantly affected by the pH of the solution.³² However, to the best of our knowledge, there have been no reports on thermoresponsive PEO-based polymers that have cloud points that can be tuned by varying the nature of the amino group or side-chain length.

As illustrated in Scheme 1, the copolymer precursor used for thiol–ene addition was synthesized via anionic ring-opening copolymerization of EO and AGE, following the procedure

reported by Lynd and co-workers.³³ Polymerization was initiated with benzyl alkoxide, which was generated by treatment of benzyl alcohol with a dilute solution of potassium naphthalenide. This method is known to be a convenient and effective method for initiating anionic ring-opening polymerization of glycidyl ethers.³⁴ The molecular weight and PDI of P(EO-*co*-AGE) were characterized by ¹H NMR spectroscopy and GPC (Figure 1 and Figure S1, S2). The number average molecular weight (*M_n*) was found to be ~6400 g·mol⁻¹ by ¹H NMR using the methylene protons of the terminal benzyl group as an internal reference (4.55 ppm). In addition, the ratio of the comonomers in the polymer backbone was determined using the characteristic allyl peaks at 5.13 and 5.22 ppm (peak *f* in Figure 1a) and 5.85 ppm (peak *e* in Figure 1a), with the results being in good agreement with the targeted value (10 mol % AGE units). The GPC of P(EO-*co*-AGE) showed a similar molecular weight to that obtained via ¹H NMR and a narrow molecular weight distribution for P(EO-*co*-AGE) (PDI = 1.10, Figure S2).

After successful polymerization of P(EO-*co*-AGE), we performed photochemical-mediated thiol–ene additions with five different aminothiols (R₁–R₅) to give the copolymers P1–P5, as shown in Scheme 1. ¹H NMR spectroscopy clearly confirmed the successful functionalization of P(EO-*co*-AGE) with different pendant amine groups that are sensitive to external pH (Figure 1). The quantitative addition of aminothiols to the P(EO-*co*-AGE) allyl groups was indicated by the disappearance of the allylic peaks from the functional AGE comonomer. The concomitant appearance of peaks corresponding to aminoalkyl groups also supported the successful conversion. GPC analyses showed narrow single peaks for P2 and P3, verifying the purity of the resulting polymers and the lack of interchain coupling (Figure S2). It should be noted that P1, P4, and P5 could not be analyzed by GPC due to the strong interactions between the pendant primary amine groups and the GPC column. Table 1 summarizes the characterization data for the PEO-based copolymers with pendant amine groups prepared through anionic ring-opening polymerization and thiol–ene addition.

The resulting polymers formed transparent aqueous solutions at room temperature due to the high aqueous solubility of the PEO backbone. Significantly, raising the temperature induced abrupt increase in turbidity, demonstrating thermally induced phase transition behavior. This allowed the thermoresponsive phase transition behaviors of the polymers to be investigated by UV–vis spectroscopy. Transmittance changes in 0.10 wt % aqueous polymer solutions as a function of temperature were measured by UV–vis spectroscopy at 500 nm, with the cloud points being defined as the temperature at which a 10% decrease in transmittance was recorded (Figure 2).^{37,38} The cloud points of P1 were 70 and 91 °C at pH 13.0 and 12.5, respectively (Figure 2a). When the pH was below 12.5, no phase transitions were observed below 100 °C, suggesting that the primary amine groups on the side chains were protonated under more acidic conditions. Consequently, P1 consists of both a hydrophilic PEO backbone and protonated amine groups below pH 12, resulting in increased solubility in water at higher temperatures. This observation was in accordance with previous reports showing the effect of hydrophobic/hydrophilic side chains on the nature of the ionizable groups.^{19,39} As shown in Figure 2b, the behavior of P2 showed significant variation, with the cloud point being 91 °C at pH 9.0 and 50 °C at pH 13.0. The LCST

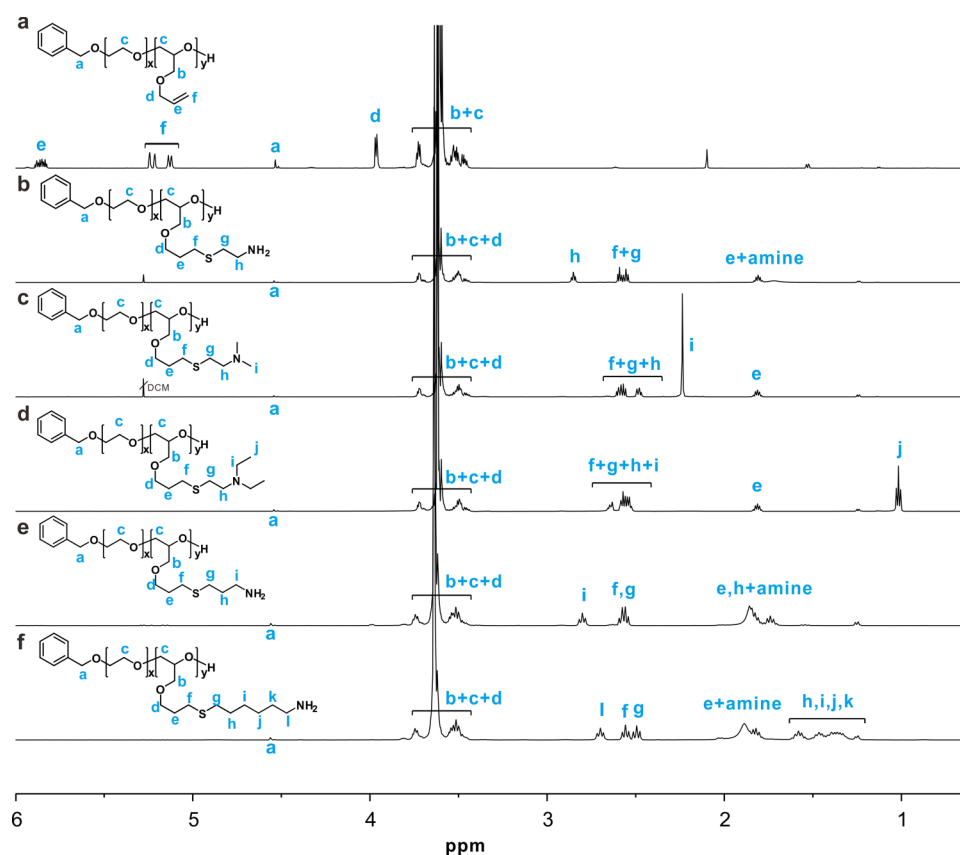


Figure 1. Representative ^1H NMR spectra of the synthesized polymers (600 MHz in CDCl_3). (a) P(EO-co-AGE), (b) **P1**, (c) **P2**, (d) **P3**, (e) **P4**, and (f) **P5**.

Table 1. Molecular Weight Data and Cloud Points of Polymers Prepared in This Study

entry	thiols	M_n^a (g/mol)/NMR	PDI ^b	cloud point ($^{\circ}\text{C}$)			log P^c
				pH 11	pH 12	pH 13	
P(EO ₁₁₇ -co-AGE ₁₁)		6400	1.10				
P1	cysteamine	6900	N/A	100	100	70	0.01
P2	<i>N,N</i> -dimethylaminoethanethiol	7800	1.10	72	63	50	1.19
P3	<i>N,N</i> -diethylaminoethanethiol	8000	1.12	65	58	45	2.34
P4	3-amino-1-propanethiol	7500	N/A	85	79	66	0.53
P5	6-amino-1-hexanethiol	7800	N/A	61	51	44	2.07

^aMolecular weight (M_n), as determined from ^1H NMR spectra of resulting polymer. ^bPDI was measured by GPC using CHCl_3 as an eluent. ^cLog P values for thiols were obtained using ALOGPS 2.1.^{35,36}

decreased with increasing pH as the balance of hydrophilicity and hydrophobicity was changed by the protonation state of the *N,N*-dimethylamino group. Figure 2c also clearly shows that the cloud point of **P3** decreased as the pH was increased from 9.0 to 13.0. The results from these three polymers show that as the amine group is changed from primary to tertiary, the cloud point of the polymer at pH 13 decreased. Although a phase transition below 100 $^{\circ}\text{C}$ was not observed for **P1** at pH 12.0, **P2** and **P3** showed clear decreases in transmittance at pH 12.0 and 11.0, suggesting that the alkyl groups on the tertiary amines enhanced their hydrophobicity, inhibiting the hydration of the protonated amine moieties. As a result, the polymers retained a hydrophobicity/hydrophilicity balance and exhibited LCST behavior at lower pH values. These observations indicate that the LCST transition is primarily affected by the hydrophobicity of the amine groups, in accordance with previous findings for other materials.⁴⁰ As further evidence, the phase transition

behavior of **P3** in Figure 2c shows that the cloud points of **P3** were lower than those of **P1** and **P2** at high pH, and that the transmittance dropped more drastically upon heating. This was likely due to the increased hydrophobicity of the diethylamino group in **P3**, which resulted in this polymer showing the lowest cloud points under basic conditions.

In order to investigate the effect of side chain hydrophobicity further, polymers with primary amine groups but different side chain lengths were examined. In this series, the cloud point of **P1**, **P4**, and **P5** were compared and analyzed according to the length of the pendant chains. Again, **P1**, **P4**, and **P5** showed pH-responsive LCST behavior due to the primary amine groups. By comparing the transmittance curves shown in Figure 2, it can be seen that the polymer with the longest side chain (**P5**) exhibited the lowest cloud point at a given pH. As the side chain length was increased from ethyl (**P1**) to propyl (**P4**) to hexyl (**P5**), the cloud point at pH 13 decreased from 70 to 66

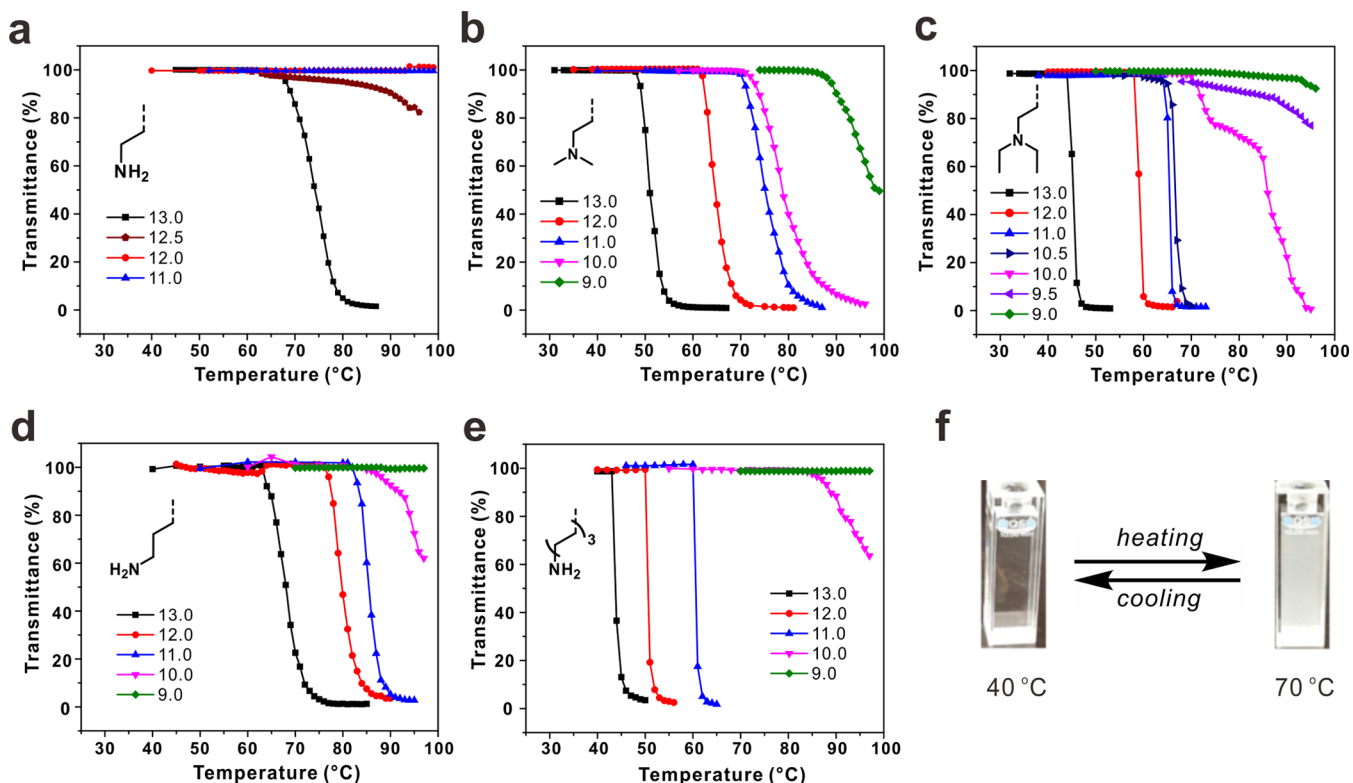


Figure 2. (a–e) Temperature-dependent transmittance curves for (a) P1, (b) P2, (c) P3, (d) P4, and (e) P5 in solutions with different pH values. (f) Turbidity change of P2 at pH 13 when cycling the temperature. All polymers were tested at a concentration of 0.10 wt %.

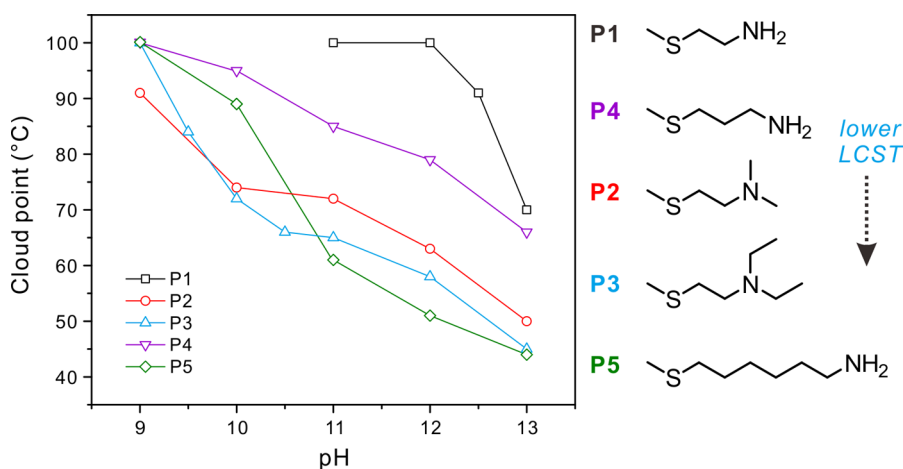


Figure 3. Summary of all cloud points for P1–P5 as a function of pH.

to and 44 °C for P1, P4, and P5, respectively. These observations indicate that the LCST transition is significantly affected by the length of the side chain. It was observed that the phase transition of P5 was reversible with a clear hysteresis occurring during the cooling process (Figure S3).

A comparison of the cloud points of the different polymers as a function of pH is shown in Figure 3, which clearly shows that the cloud point at a given pH decreased as the hydrophobicity of the amine group or length of the side chain was increased. To quantitatively investigate the effect of side chain hydrophobicity, the octanol/water coefficients ($\log P$) of the thiols (R_1 – R_5) were calculated using the software ALOGPS 2.1, based on a well-known computational model (Table 1).^{35,36} Comparing the $\log P$ values of the side chain of P1, P2, and P3,

it can be seen that the hydrophobicity increased as the number of carbons on the N atom increased. Increasing the hydrophobicity of the amine moiety significantly lowered the cloud points at all pH values. As expected, the side chain length was also highly correlated with hydrophobicity, as can be seen by comparing the $\log P$ values of P1, P4, and P5.

Despite these relationships, comparing the $\log P$ values of P3 and P5 shows there was not an exact correlation between cloud point and hydrophobicity. It should be noted that P3 and P5 have the same number of carbons on their side chains. Nevertheless, the $\log P$ values of P3 and P5 are 2.34 and 2.07, respectively, indicating that P3 was more hydrophobic than P5. However, the cloud point of P3 was higher than P5 between pH 11.0 and 13.0, suggesting that the primary amine group on

PS can collapse into a globule state at lower temperatures due to intra/interchain hydrogen bonds.⁴¹ As shown in Figure S3, the hysteresis is observed clearly in a heating-and-cooling cycle, attributed to the formation of additional hydrogen bonds of each primary amine groups that inhibits hydration in the cooling process. The LCST trends of P3 and P5 reversed below pH 11.0, as protonated primary amines can be hydrated much more easily than the protonated tertiary amines due to the hydrophobic diethyl groups that inhibit interaction with water. It can therefore be concluded that LCST-type phase transition is affected by a complicated interaction of the hydrophilicity/hydrophobicity balance with hydrogen bonding ability.

In summary, the pH-responsive LCST behavior of PEO-based functional polymers with different pendant amine groups and varying side chain lengths has been investigated. Five different aminothiols, including cysteamine, *N,N*-dimethylaminoethanethiol, *N,N*-diethyl aminoethanethiol, 3-amino-1-propanethiol, and 6-amino-1-hexanethiol could be quantitatively introduced to a single, well-defined P(EO-*co*-AGE) copolymer starting material via facile and modular thiol-ene chemistry. The transmission spectra for aqueous solutions of these copolymers revealed that cloud point was not only tuned by the pH of the solution but also by the hydrophobicity of the pendant amine moieties. The polymer library also exhibited different thermoresponsive phase transition behavior depending on the side chain length with the hydrophilicity/hydrophobicity balance being the dominant factor in controlling LCST behavior. By designing pH-tunable, thermoresponsive PEO-based polymers with multiple types of amine and different chain lengths, an effective and facile method of controlling LCST behavior has been developed. This fundamental and systematic investigation provides a platform to understand a wide range of LCST behaviors.

■ ASSOCIATED CONTENT

Supporting Information

The Supporting Information is available free of charge on the ACS Publications website at DOI: 10.1021/acsmacrolett.6b00830.

Detailed experimental procedures and additional ¹H NMR and GPC data (PDF).

■ AUTHOR INFORMATION

Corresponding Authors

*E-mail: hawker@mrl.ucsb.edu.

*E-mail: bskim19@unist.ac.kr.

ORCID

Joonhee Lee: 0000-0002-6043-6821

Byeong-Su Kim: 0000-0002-6419-3054

Notes

The authors declare no competing financial interest.

■ ACKNOWLEDGMENTS

This work was supported by the 2016 UNIST Research Fund (1.160001.01) and by the National Research Foundation of Korea (NRF; 2010-0028684). Funding is also acknowledged from the Institute for Collaborative Biotechnologies through Grant W911NF-09-0001 from the U.S. Army Research Office (A.M. and C.J.H.) with facilities support from the National Science Foundation (Materials Research Laboratory, DMR-1121053). The content of the information does not necessarily

reflect the position or the policy of the U.S. government, and no official endorsement should be inferred.

■ REFERENCES

- (1) Congdon, T.; Shaw, P.; Gibson, M. I. *Polym. Chem.* **2015**, *6*, 4749–4757.
- (2) Jiang, X.; Feng, C.; Lu, G.; Huang, X. *ACS Macro Lett.* **2014**, *3*, 1121–1125.
- (3) Tang, Z.; Wilson, P.; Kempe, K.; Chen, H.; Haddleton, D. M. *ACS Macro Lett.* **2016**, *5*, 709–713.
- (4) Lee, A.; Lundberg, P.; Klinger, D.; Lee, B. F.; Hawker, C. J.; Lynd, N. A. *Polym. Chem.* **2013**, *4*, 5735.
- (5) Son, S.; Shin, E.; Kim, B.-S. *Biomacromolecules* **2014**, *15*, 628–634.
- (6) Davis, D. A.; Hamilton, A.; Yang, J.; Cremer, L. D.; Van Gough, D.; Potisek, S. L.; Ong, M. T.; Braun, P. V.; Martinez, T. J.; White, S. R.; Moore, J. S.; Sottos, N. R. *Nature* **2009**, *459*, 68–72.
- (7) Pang, Y.; Zhu, Q.; Zhou, D.; Liu, J.; Chen, Y.; Su, Y.; Yan, D.; Zhu, X.; Zhu, B. J. *Polym. Sci., Part A: Polym. Chem.* **2011**, *49*, 966–975.
- (8) Kojima, C.; Yoshimura, K.; Harada, A.; Sakanishi, Y.; Kono, K. *Bioconjugate Chem.* **2009**, *20*, 1054–1057.
- (9) Zhang, H.; Guo, S.; Fan, W.; Zhao, Y. *Macromolecules* **2016**, *49*, 1424–1433.
- (10) Zhu, Y.; Batchelor, R.; Lowe, A. B.; Roth, P. J. *Macromolecules* **2016**, *49*, 672–680.
- (11) Smith, G. D.; Bedrov, D. J. *Phys. Chem. B* **2003**, *107*, 3095–3097.
- (12) Hou, L.; Wu, P. *Soft Matter* **2014**, *10*, 3578–3586.
- (13) Lutz, J.-F.; Akdemir, Ö.; Hoth, A. J. *Am. Chem. Soc.* **2006**, *128*, 13046–13047.
- (14) Lutz, J.-F.; Hoth, A. *Macromolecules* **2006**, *39*, 893–896.
- (15) Lutz, J.-F.; Weichenhan, K.; Akdemir, Ö.; Hoth, A. *Macromolecules* **2007**, *40*, 2503–2508.
- (16) Min, S. H.; Kwak, S. K.; Kim, B.-S. *Soft Matter* **2015**, *11*, 2423–2433.
- (17) Yamamoto, S.; Pietrasik, J.; Matyjaszewski, K. *Macromolecules* **2008**, *41*, 7013–7020.
- (18) Lei, L.; Zhang, Q.; Shi, S.; Zhu, S. *ACS Macro Lett.* **2016**, *5*, 828–832.
- (19) Jiang, X.; Feng, C.; Lu, G.; Huang, X. *ACS Macro Lett.* **2014**, *3*, 1121–1125.
- (20) Kohsaka, Y.; Matsumoto, Y.; Kitayama, T. *Polym. Chem.* **2015**, *6*, 5026–5029.
- (21) Fruijtier-Pöloth, C. *Toxicology* **2005**, *214*, 1–38.
- (22) Fuertges, F.; Abuchowski, A. J. *Controlled Release* **1990**, *11*, 139–148.
- (23) Pelegri-O'Day, E. M.; Lin, E.-W.; Maynard, H. D. *J. Am. Chem. Soc.* **2014**, *136*, 14323–14332.
- (24) Saeki, S.; Kuwahara, N.; Nakata, M.; Kaneko, M. *Polymer* **1976**, *17*, 685–689.
- (25) Aoki, S.; Koide, A.; Imabayashi, S.; Watanabe, M. *Chem. Lett.* **2002**, *31*, 1128–1129.
- (26) Müller, S. S.; Moers, C.; Frey, H. *Macromolecules* **2014**, *47*, 5492–5500.
- (27) Mangold, C.; Dingels, C.; Obermeier, B.; Frey, H.; Wurm, F. *Macromolecules* **2011**, *44*, 6326–6334.
- (28) Mangold, C.; Obermeier, B.; Wurm, F.; Frey, H. *Macromol. Rapid Commun.* **2011**, *32*, 1930–1934.
- (29) Obermeier, B.; Wurm, F.; Frey, H. *Macromolecules* **2010**, *43*, 2244–2251.
- (30) Obermeier, B.; Frey, H. *Bioconjugate Chem.* **2011**, *22*, 436–444.
- (31) Jain, K.; Vedarajan, R.; Watanabe, M.; Ishikiriyama, M.; Matsumi, N. *Polym. Chem.* **2015**, *6*, 6819–6825.
- (32) Jung, S.-H.; Song, H.-Y.; Lee, Y.; Jeong, H. M.; Lee, H. *Macromolecules* **2011**, *44*, 1628–1634.
- (33) Lee, B. F.; Wolffs, M.; Delaney, K. T.; Sprafke, J. K.; Leibfarth, F. A.; Hawker, C. J.; Lynd, N. A. *Macromolecules* **2012**, *45*, 3722–3731.

(34) Lee, B. F.; Kade, M. J.; Chute, J. A.; Gupta, N.; Campos, L. M.; Fredrickson, G. H.; Kramer, E. J.; Lynd, N. A.; Hawker, C. J. *J. Polym. Sci., Part A: Polym. Chem.* **2011**, *49*, 4498–4504.

(35) Tetko, I. V.; Gasteiger, J.; Todeschini, R.; Mauri, A.; Livingstone, D.; Ertl, P.; Palyulin, V. A.; Radchenko, E. V.; Zefirov, N. S.; Makarenko, A. S.; Tanchuk, V. Y.; Prokopenko, V. V. *J. Comput.-Aided Mol. Des.* **2005**, *19*, 453–463.

(36) VCCLAB, Virtual Computational Chemistry Laboratory; <http://www.vcclab.org>, 2005.

(37) Kawaguchi, T.; Kojima, Y.; Osa, M.; Yoshizaki, T. *Polym. J.* **2008**, *40*, 455–459.

(38) Koda, Y.; Terashima, T.; Sawamoto, M. *ACS Macro Lett.* **2015**, *4*, 1366–1369.

(39) Dimitrov, I.; Trzebicka, B.; Müller, A. H. E.; Dworak, A.; Tsvetanov, C. B. *Prog. Polym. Sci.* **2007**, *32*, 1275–1343.

(40) Aoshima, S.; Oda, H.; Kobayashi, E. *J. Polym. Sci., Part A: Polym. Chem.* **1992**, *30*, 2407–2413.

(41) Cheng, H.; Shen, L.; Wu, C. *Macromolecules* **2006**, *39*, 2325–2329.